Material Properties of a Sintered α-SiC

Cite as: Journal of Physical and Chemical Reference Data **26**, 1195 (1997); https://doi.org/10.1063/1.556000
Submitted: 19 February 1997 . Published Online: 15 October 2009

R. G. Munro

Material Properties of a Sintered α-SiC

R. G. Munro

Ceramics Division, National Institute of Standards and Technology, Gaithersburg, Maryland 20899

Received February 19, 1997; revised manuscript received May 20, 1997

A self-consistent, single-valued representation of the major physical, mechanical, and thermal properties of a sintered α-SiC is presented. This comprehensive set of properties is achieved by focusing on a narrowly defined material specification in which boron and carbon are used as sintering aids to produce a dense ceramic ($\geqslant$98% of the theoretical maximum density) with a grain size of (6 ± 2) μm. Such a representation is highly desirable in applications of concurrent engineering practices and for the increasing use of electronic processing of product specifications. © *1997 American Institute of Physics and American Chemical Society.* [S0047-2689(97)00105-0]

Key words: evaluated data; mechanical properties; physical properties; silicon carbide; thermal properties.

Contents

1. Introduction. 1195
2. Material Specification. 1196
3. Properties and Characteristics. 1196
   3.1 Crystallography, Density,and Thermal Expansion. 1196
   3.2 Elastic Properties. 1197
   3.3 Strength and Related Properties. 1198
   3.4 Creep Characteristics. 1199
   3.5 Tribological Characteristics. 1200
   3.6 Thermal Properties. 1200
4. Conclusion. 1202
5. References. 1202

List of Tables

1. Bend test configurations for flexural strength measurements. 1198
2. Test configurations and conditions in the friction and wear studies for Fig. 12. 1201
3. Evaluated property values for sintered α-SiC. . . . 1202

List of Figures

1. The lattice parameters of silicon carbide polytype 6H: (a) a axis, (b) c axis.. 1196
2. The thermal expansion of sintered α-SiC: (a) cumulative expansion coefficient, (b) density.. . . . 1197
3. The elastic properties of sintered α-SiC: (a) moduli, (b) Poisson's ratio, (c) sound velocities... 1197
4. The flexural strength of sintered α-SiC in four-point and three-point bending.. 1198
5. The Weibull modulus of sintered α-SiC in four-point bending.. 1198
6. The tensile strength of sintered α-SiC.. 1198
7. The Vickers hardness of sintered α-SiC.. 1199
8. The fracture toughness of sintered α-SiC by surface crack in flexure methods.. 1199
9. The creep rate of sintered α-SiC in flexure, tension, and compression.. 1199
10. Arrhenius type plot of the creep rate under three different stress levels.. 1200
11. The creep rate of sintered α-SiC under compression with the solid curves obtained from Eq. (10) and the parameters given in the text.. . . . 1200
12. Wear of sintered α-SiC when the load is $\leqslant$10 N, the sliding speed is $\leqslant$0.25 m/s; (a) friction and (b) wear coefficient.. 1201
13. The specific heat of a variety of sintered α-SiC materials.. 1201
14. Transport properties for sintered α-SiC materials; (a) thermal conductivity, (b) thermal diffusivity... 1201

1. Introduction

The primary concern in the use of advanced ceramics in structural applications has continued to be the issue of reliability.[1,2] In the past, it has not been unusual that different batches of a given material prescription would yield measurably distinct characteristics. More recently, however, the production characteristics of several advanced ceramic materials have matured sufficiently that their material properties are routinely reproducible as judged by the consistency of numerous studies in independent laboratories. Furthermore, progress in concurrent engineering[3] and electronic product design tools such as the evolving Standard for the Exchange of Product Data (STEP)[4] has increased the need for well defined data sets. Consequently, it has become meaningful and desirable to construct and assess comprehensive sets of properties that characterize these materials. Towards that end, the present article examines the material properties of one specification of a sintered α-SiC.

Sintered α-SiC has evolved as a major structural ceramic with applications that include heat exchangers for high temperature and aggressive environments, seals, bearings, and

wear resistant components. Several reviews[5–9] of the properties of silicon carbide have contributed to this evolution by delineating the ranges of performance characteristics that can be expected for this general class of materials. The present work refines those previous efforts by developing a comprehensive set of properties for a single material specification; the properties presented here form a coherent unit that provides a self-consistent, single-valued representation of the observed performance characteristics of that material. Such a representation is highly desirable in applications of concurrent engineering practices and for the increasing use of electronic processing of product specifications.

2. Material Specification[a]

Sintered α-SiC ceramics typically are produced using submicrometer powders that have been extracted from an Acheson furnace and ground to a fine particle size. Boron and carbon are used as sintering aids to achieve improved densification during sintering which is typically conducted at a temperature on the order of 2500 °C. The resulting microstructure consists predominantly of fine, equiaxed grains of the hexagonal SiC polytype 6H. A small amount of free carbon and isolated B_4C grains may be present also as remnant artifacts of the sintering aids.

Since the properties of ceramics can vary significantly with composition and microstructure, it is important to restrict attention to a consistently defined material specification. In the present exercise, the material specification is patterned after a commercial material, Hexoloy SA™, abbreviated here as SA, for which a considerable amount of data can be gleaned from numerous independent studies. For this material,[10,11] the density is approximately $(98\pm1)\%$ of the density of single crystal SiC(6H) with a mean grain size of (6 ± 2) μm. The mass fractions of boron and free carbon in the sintered composition are $(0.4\pm0.1)\%$ and $(0.5\pm0.1)\%$, respectively. The combined standard uncertainties[12] for these values are estimated using the standard deviation of the respective reported values.

3. Properties and Characteristics

The emphasis in this work is on the variation of the properties with temperature, and the primary objective is to obtain a coherent, self-consistent representation of the material in terms of the collection of assessed properties. Whenever feasible and appropriate, analytical expressions are provided to serve as useful interpolation formulas. Combined standard uncertainties for the properties are estimated using the standard deviations or standard errors of the respective property values.[12]

[a]Certain commercial names are identified in this article for the purpose of clarity in the presentation. Such identification does not imply recommendation or endorsement by the National Institute of Standards and Technology.

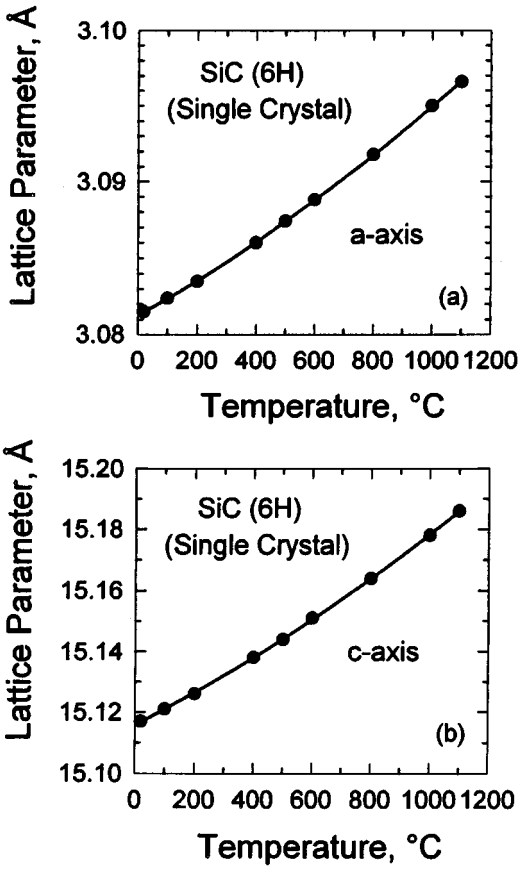

FIG. 1. The lattice parameters of silicon carbide polytype 6H: (a) a axis, (b) c axis.

3.1. Crystallography, Density, and Thermal Expansion

The predominant phase of the constituent grains of sintered α-SiC is the hexagonal 6H structure. The lattice parameters[13] as a function of temperature are shown in Fig. 1. There is a slight curvature in the trend lines for both of the a and c lattice parameters which may be well represented by a second order polynomial in the temperature:

$$a(\text{Å}) = 3.0813 + 1.0816\cdot10^{-5}T + 2.8833\cdot10^{-9}T^2 \pm 0.01\%, \quad (1a)$$

$$c(\text{Å}) = 15.116 + 5.104\cdot10^{-5}T + 1.153\cdot10^{-8}T^2 \pm 0.02\%, \quad (1b)$$

where the temperature is in the range $0\,°\text{C} \leqslant T \leqslant 1100\,°\text{C}$. These results permit the density, ρ_{6H}, of the single crystal specimen to be calculated from the relation

$$\rho_{6H} = \frac{Mn}{N_A V}, \quad (2)$$

where M is the molecular weight, n is the number of formula units per unit cell, N_A is Avogadro's number, and V is the unit cell volume. For SiC(6H), $M=40.097$, $n=6$, and $V=(3/4)^{1/2}\ a^2c$, and at 20 °C, $\rho_{6H}=(3.214\pm0.001)$ g/cm^3. The density ρ_{6H} is theoretically the maximum density that a pure sintered material could attain. In practice, the density of

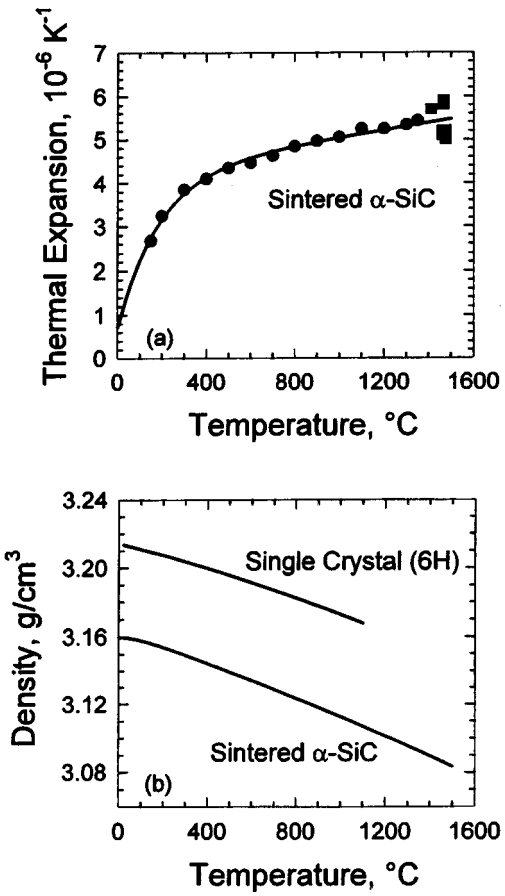

FIG. 2. The thermal expansion of sintered α-SiC: (a) cumulative expansion coefficient, (b) density.

a single phase polycrystalline material should be less than the theoretical density. In the present work, no report of the temperature dependence of the density of sintered α-SiC was found. However, several measurements of the density of SA at room temperature have been reported, and measurements of the isotropic thermal expansion to several temperatures have been reported. These results can be combined to yield the variation of the density with temperature,

$$\rho(T)=\rho_0[1+\alpha_{m,c}(T)\cdot(T-T_0)]^{-3}, \tag{3}$$

where ρ_0 is the density at the reference temperature T_0, and $\alpha_{\mathrm{m,c}}=(2\alpha_{\mathrm{a}}+\alpha_{\mathrm{c}})/3$ is the mean cumulative linear expansion coefficient for the hexagonal material, with

$$\alpha_L(T)=\frac{1}{L_0}\left(\frac{L(T)-L_0}{T-T_0}\right), \tag{4a}$$

where L is a linear dimension and $L_0=L(T_0)$. The results[14,15] for the cumulative expansion coefficient for SA, Fig. 2(a), can be represented by the expression

$$\alpha_{m,c}(10^{-6}K^{-1})=4.22+8.33\cdot10^{-4}T-3.51e^{-0.00527T}\pm10\%, \tag{4b}$$

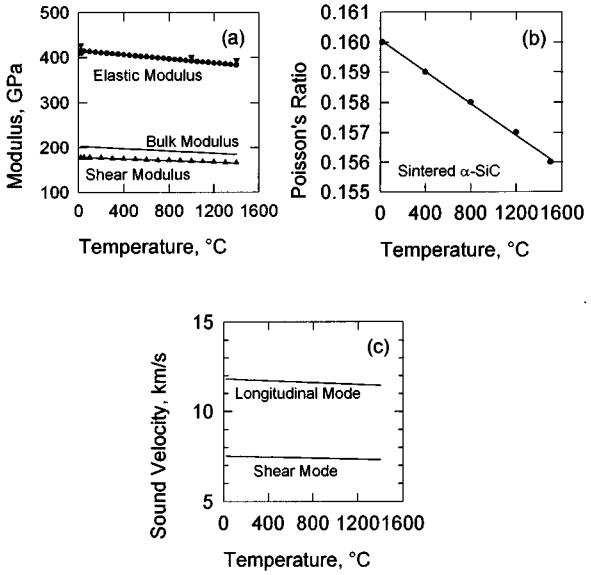

FIG. 3. The elastic properties of sintered α-SiC: (a) moduli, (b) Poisson's ratio, (c) sound velocities.

where $T_0=0$ °C, and 0 °C$\leqslant T\leqslant$1500 °C. Combining this result with the density of SA[16–20] at 0 °C, $\rho_0=(3.16\pm0.03)$ g/cm^3, yields the temperature dependence of the density, Fig. 2(b).

3.2. Elastic Properties

Structural ceramics are relatively stiff materials whose elastic properties exhibit relatively weak temperature dependencies, and the polycrystalline sintered specimens tend to have isotropic elastic moduli. For the latter case, the elastic modulus (E), shear modulus (G), bulk modulus (B), and Poisson's ratio (ν) satisfy the relations

$$G=\frac{E}{2(1+\nu)}, \tag{5a}$$

$$B=\frac{E}{3(1-2\nu)} \tag{5b}$$

for isotropic conditions. Additionally, these properties may be expressed in terms of the shear (V_{S}) and longitudinal (V_{L}) sound velocities and the density:

$$G=\rho V_{\mathrm{S}}^2 \tag{6a}$$

$$B=\rho[V_{\mathrm{L}}^2-(4/3)V_{\mathrm{S}}^2], \tag{6b}$$

where V_{S} and V_{L} are commonly determined by ultrasonic techniques. For SA, results from both ultrasonic[19–21] and resonance techniques[22] have been reported and are shown together in Figs. 3(a), 3(b), and 3(c). The interpolation formulas for E and ν are

$$E(\mathrm{GPa})=415-0.023T\pm3\%, \tag{7a}$$

$$\nu=0.160-2.62\cdot10^{-6}T\pm25\% \tag{7b}$$

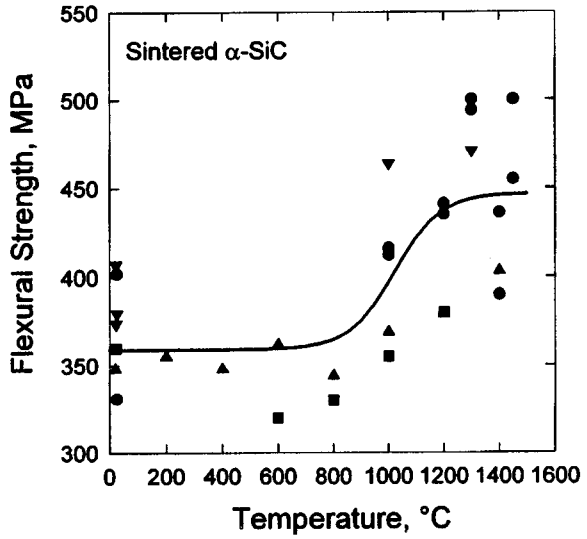

FIG. 4. The flexural strength of sintered α-SiC in four-point and three-point bending.

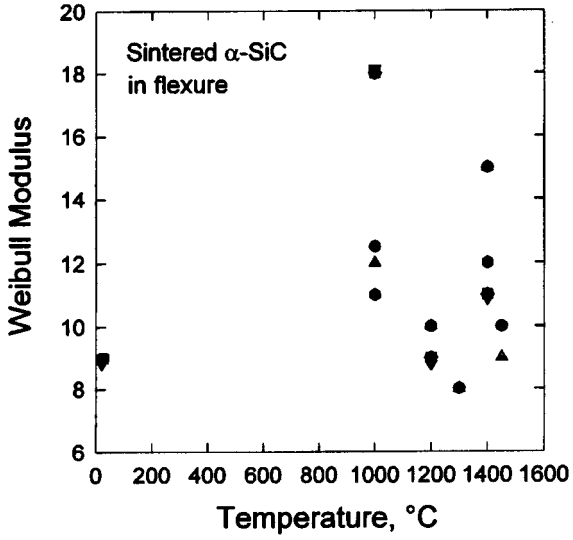

FIG. 5. The Weibull modulus of sintered α-SiC in four-point bending.

for 0 °C$\leqslant T \leqslant$1400 °C. The curves in Figs. 3(a), 3(b), and 3(c) are obtained *via* Eqs. (5)–(7).

3.3. Strength and Related Properties

The list of compelling reasons for using advanced ceramics in structural applications includes high temperature strength and high hardness. The most significant deterrent to their use is low fracture toughness. These characteristics are represented by the flexural and tensile strengths, Weibull modulus, hardness, and toughness properties.

Sintered α-SiC exhibits the somewhat unusual behavior of increasing flexural strength with increasing temperature (Fig. 4) when tests are conducted in an air environment.[16,19,23,24] This phenomenon is generally attributed to short-term crack healing[25] as a result of the formation of an oxide, SiO_2, on the surface of the silicon carbide specimen. For other environments and long-term exposures, the strength may be expected to diminish.[26] The results shown in Fig. 4 were obtained by a variety of bend test configurations (Table 1) but the collection is sufficiently consistent that a useful interpolation formula may be given as

$$\mathrm{FS(MPa)} = 359 + \frac{87.6}{1 + 208600\ \mathrm{e}^{-0.012T}} \pm 15\%, \quad (8)$$

where FS is the flexural strength and 0 °C$\leqslant T \leqslant$1500 °C.

Interestingly, the Weibull modulus (Fig. 5) is less well defined. In the temperature range of 0 °C–1500 °C, the data are not sufficient to establish a temperature dependent trend; consequently, the Weibull modulus can best be expressed as an average value, 11 ± 3.

The amount of data available on the tensile strength[19] of SA (Fig. 6) is quite limited. Those data indicate that a small increase in tensile strength may occur as the temperature is raised from 0 °C to 1400 °C, but the increase is less than the uncertainty of the measured values. Hence, the tensile strength is well represented as (250 ± 15) MPa over the observed temperature range.

TABLE 1. Bend test configurations for flexural strength measurements

Reference	Test method	Specimen sizes (mm×mm ×mm)	Outer/Inner spans (mm/mm)	Stressing rate (mm/s)
16	Four-point bend	3.18×6.35×51	38/19	0.0085
19	Four-point bend	3.2×6.4×51	38.1/19	0.0004 to 0.064
23	Four-point bend	2.5×5.0×50	19.5/6.25	100 MPa/s
24	Three-point bend	3×3×30	20	0.000167

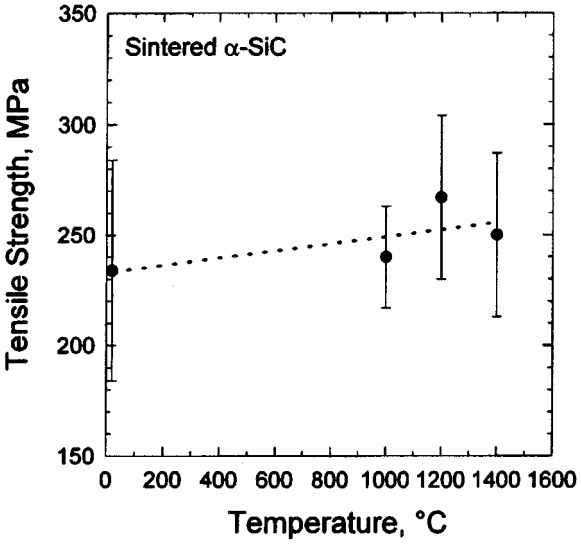

FIG. 6. The tensile strength of sintered α-SiC.

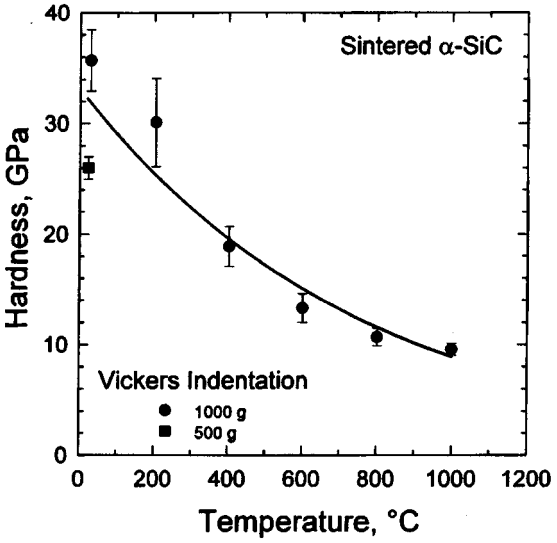

FIG. 7. The Vickers hardness of sintered α-SiC.

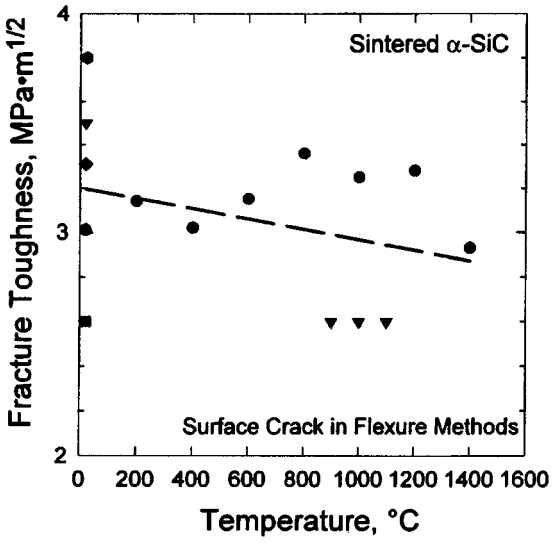

FIG. 8. The fracture toughness of sintered α-SiC by surface crack in flexure methods.

The hardness[19,27] of SA determined by the Vickers indentation method (Fig. 7) exhibits an exponential temperature dependence. The solid curve for the hardness, H, in Fig. 7 is given by

$$H(\mathrm{GPa}) = 33\ \mathrm{e}^{-0.0013T} \pm 15\%, \tag{9}$$

where $0\ ^\circ\mathrm{C} \leqslant T \leqslant 1000\ ^\circ\mathrm{C}$.

The fracture toughness of SA has been studied by a large variety of measurement methods.[20,21,24,28–34] The results vary considerably among the distinct methods, but several independent studies have concluded that sharp crack techniques provide the more reliable results. An international round-robin study,[35] in particular, has demonstrated that consistent interlaboratory results for brittle ceramics can be obtained from the surface crack in flexure (SCF) method. This method is also known as the controlled surface flaw or controlled microflaw method. Results[20,24,30–33] from SCF type measurements are shown in Fig. 8. The latter data yield a temperature-independent value of 3.1 ± 0.3 MPa $\mathrm{m}^{1/2}$ for this sintered α-SiC.

3.4. Creep Characteristics

The operation of structural ceramics for long times under loads at high temperatures is limited by the creep characteristics of the material. The steady state creep rate, $\mathrm{d}\epsilon/\mathrm{d}t$, of a structural ceramic is generally of the form

$$\mathrm{d}\epsilon/\mathrm{d}t = A\sigma^n\ \mathrm{e}^{-E_{\mathrm{act}}/RT}, \tag{10}$$

where the independent variables are stress, σ, and the absolute temperature, T; $R = 8.3145$ J/(mol K); and A, n, and E_{act} are parameters to be determined from the data. The parameter n is called the creep stress exponent, and E_{act} is the creep activation energy.

The creep rates of SA (Fig. 9) in flexure,[36] tension,[37] and compression[17] are of the same order of magnitude, 10^{-9} s^{-1}, at 1500 °C. The results in flexure and compression suggest that the stress dependence in each case is somewhat greater than linear, i.e., $n > 1$ in both flexure and compression. The temperature dependence of the creep rate under compression has a more interesting character. The trend lines at intervals of 50 °C have a significantly different spacing in Fig. 9 at low and high temperatures, unlike what would be expected from Eq. (10). These differences become very clear when the results for three different values of the applied stress are examined in an Arrhenius type plot (Fig. 10). In the latter figure, there is a clear distinction between the results from above and below 1600 °C, suggesting a significant change in the creep mechanism at that temperature. In the context of Eq. (10), this result suggests that there are two distinct activation energies. Accordingly, assuming two acti-

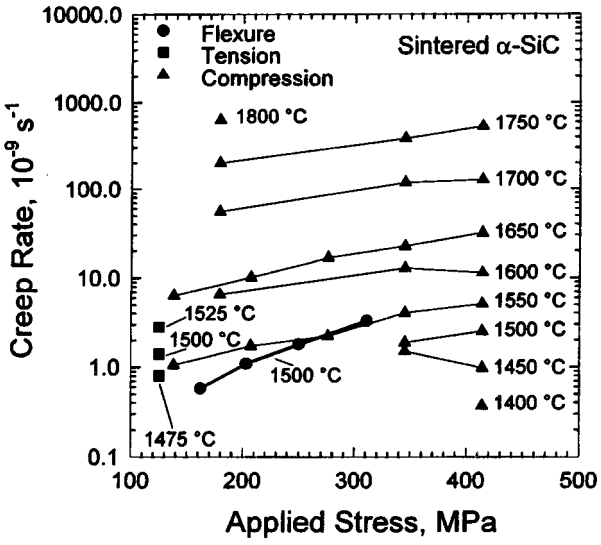

FIG. 9. The creep rate of sintered α-SiC in flexure, tension, and compression.

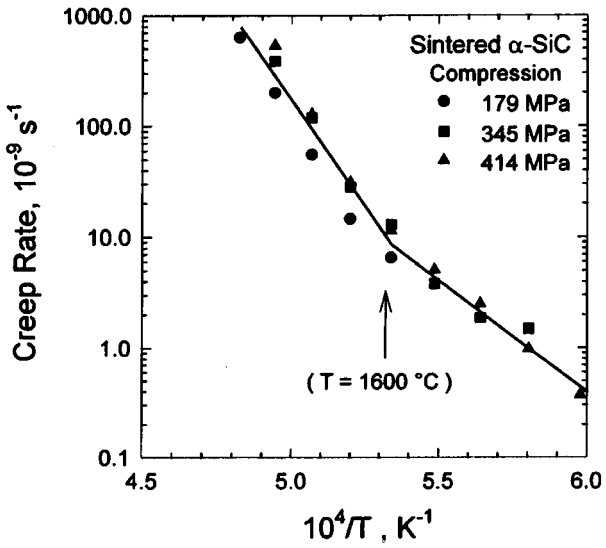

FIG. 10. Arrhenius type plot of the creep rate under three different stress levels.

vation energies, the creep data under compression can be well represented by Eq. (10) (Fig. 11) with the values of the parameters being $A=7.35\ \mathrm{s}^{-1}\ \mathrm{MPa}^{-1.36}$, $n=1.36$, $E_{\mathrm{act}}=442$ kJ/mol for $T\leqslant 1600$ °C; and $A=4.5\times 10^{14}\ \mathrm{s}^{-1}\ \mathrm{MPa}^{-1.32}$, $n=1.32$, $E_{\mathrm{act}}=944$ kJ/mol for $T>1600$ °C. These parameters yield an estimated combined standard uncertainty of 17% for the creep rate.

3.5. Tribological Characteristics

An increasing number of the applications of structural ceramics involve sliding wear conditions.[38] In these applications, friction and wear characteristics are important factors in the assessment of the impact of the materials on the application's lifetime and operating costs. Definitive measurements of these characteristics, however, are difficult to achieve because the pertinent interactions involve nonequilibrium thermodynamics, chemical reactions under rapidly varying localized temperatures, stresses, and stress gradients, and catastrophic mechanical collisions of macroscopic and microscopic surface features. Laboratory results for friction and wear, therefore, may depend significantly on both the design of the measurement apparatus and the specific procedure that is applied to the measurement. Early considerations of this variability in results led to the use of a normalized, dimensionless measure of wear,[39]

$$K_{\mathrm{W}}=\frac{V_{\mathrm{W}}H}{F_{\mathrm{n}}D_{\mathrm{s}}}, \tag{11}$$

where K_{W} is called the wear coefficient, V_{W} is the wear volume, H is the hardness, F_{n} is the normal force, and D_{s} is the total sliding distance. The wear coefficient and the dimensionless coefficient of friction (COF) are used together with microscopy and spectroscopy techniques to delineate reasonably distinct regions of wear mechanisms and performance levels.[40]

Results for brittle materials show a considerable amount of scatter which makes the identification of trends in the data somewhat tenuous. Comparisons of dry friction and wear results from different studies are particularly difficult, and attention must be given to the test conditions to ensure that the tests have comparable loads, sliding speeds, and environmental conditions. Results from four different studies[27,41–43] of sintered α-SiC under dry sliding conditions, involving four different sources of the test materials, are shown together in Fig. 12, while the test conditions are described in Table 2. The wear coefficient from all of these studies may be cited as $K_{\mathrm{W}}=(2.5\pm 2)\times 10^{-4}$ when the sliding speed is $\leqslant 0.3$ m/s, the load is $\leqslant 10$ N, and the temperature is in the range $0\ ^{\circ}\mathrm{C}\leqslant T\leqslant 1000\ ^{\circ}\mathrm{C}$. There may be a small initial increase in K_{W} as the temperature increases from room temperature, but the apparent increase is smaller than the uncertainty in the property value. Concurrently, the COF appears to have a value of 0.7 ± 0.15 for $T<250$ °C and 0.4 ± 0.1 for $T>250$ °C. Examinations of the microstructure suggest[27] that the higher friction region with $T<250$ °C is a result of the ploughing wear of the surface, while for $T>250$ °C, the formation of mixed oxides on the surface reduce the effective coefficient of friction. When the load is increased above 10 N, however, the order of magnitude of K_{W} increases to 10^{-3}, and the wear behavior becomes considerably more complicated and involves microfracture and compacted wear debris.

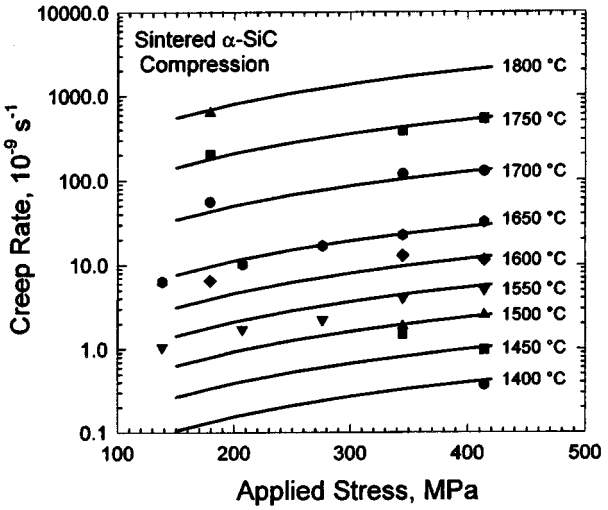

FIG. 11. The creep rate of sintered α-SiC under compression with the solid curves obtained from Eq. (10) and the parameters given in the text.

3.6. Thermal Properties

There are three thermal properties that are particularly important for the application of ceramics at high temperature, specific heat, thermal conductivity, and thermal diffusivity, which are related respectively to the absorption of heat, the steady state transport of heat, and the transient response to heat fluctuations. For isotropic materials, these quantities satisfy the relation

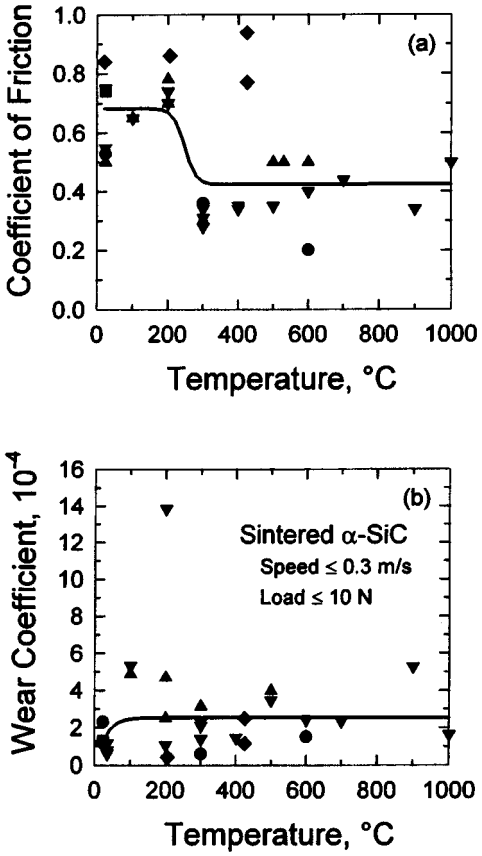

FIG. 12. Wear of sintered α-SiC when the load is $\leqslant$10 N, the sliding speed is $\leqslant$0.25 m/s; (a) friction and (b) wear coefficient.

$$\kappa = \rho C_p D, \tag{12}$$

where κ is the thermal conductivity, ρ is the mass density, C_p is the specific heat at constant pressure, and D is the thermal diffusivity.

The specific heat of sintered α-SiC for T$\geqslant$0 °C is not particularly sensitive to variations in its minor constituents, as shown by the collection of results[44–48] in Fig. 13. Consequently, the specific heat of SA should be well represented by the smooth curve in Fig. 13, which is given by the interpolation formula

$$C_p(Jkg^{-1}K^{-1}) = 1110 + 0.15T - 425\ e^{-0.003T} \pm 5\% \tag{13}$$

for $0 \leqslant T \leqslant 2000$ °C.

In contrast, the thermal transport properties can be expected to depend on composition and microstructural details.

TABLE 2. Test configurations and conditions in the friction and wear studies for Fig. 12

Reference	Configuration	Load (N)	Sliding speed (m/s)
27	Pin on disk, reciprocating	4.9	0.0014
33	Pin on disk, reciprocating	9	0.3
34	Ring on flat, unidirectional	10	0.2
35	Cylinder on flat, unidirectional (also called roller on beam)	10	0.25

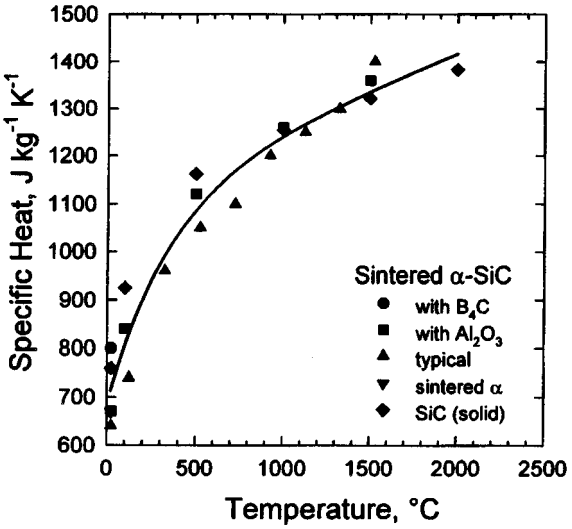

FIG. 13. The specific heat of a variety of sintered α-SiC materials.

Results for thermal conductivity[21,49,50] and thermal diffusivity[49,51] for SA are shown in Fig. 14. The interpolation formulas for κ and D were determined simultaneously using these data with Eq. (12), the density from Eq. (3), and the specific heat from Eq. (13):

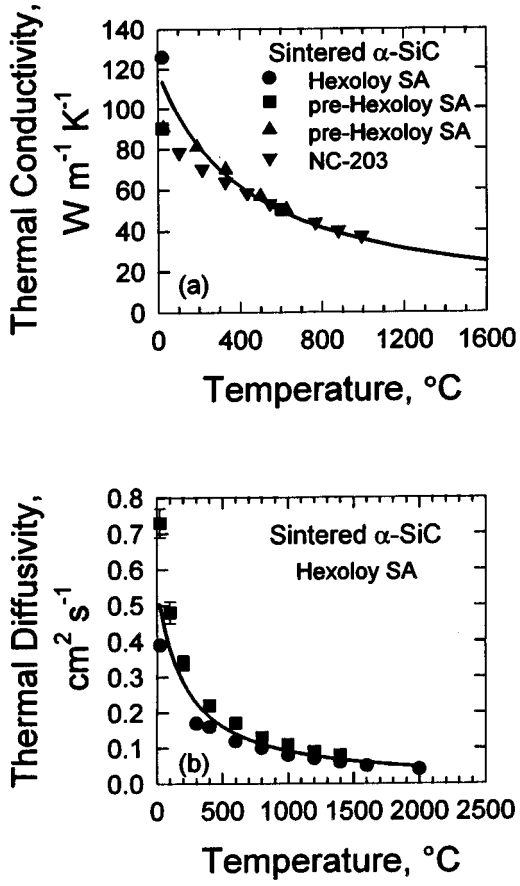

FIG. 14. Transport properties for sintered α-SiC materials; (a) thermal conductivity, (b) thermal diffusivity.

TABLE 3. Evaluated property values for sintered α-SiC; sintering aids (mass fractions): B(0.4%) and C (0.5%); mass density ≥98% of the theoretical density; nominal grain size=(6±2) μm. Percentages in parentheses are estimated relative combined standard uncertainties; i.e., the quantity 3.0(5%) is equivalent to 3.0±0.15. Property values in parentheses are extrapolated values. Units are given within square brackets [ ]

Property [unit]	20 °C	500 °C	1000 °C	1200 °C	1400 °C	1500 °C
Bulk modulus [GPa]	203 (3%)	197	191	188	186	184
Creep rate [10^{-9} s^{-1}] at 300 MPa	0	0	0	0.004 (17%)	0.27	1.6
Density [g/cm^3]	3.16 (1%)	3.14	3.11	3.10	3.09	3.08
Elastic modulus [GPa]	415(3%)	404	392	387	383	380
Flexural strength [MPa]	359(15%)	359	397	437	446	446
Fracture toughness [MPa $m^{1/2}$]	3.1(10%)	3.1	3.1	3.1	3.1	3.1
Friction coefficient [ ] at 0.2 m/s, 5 N	0.7(21%)	0.4	0.4			
Hardness (Vickers, 1 kg) [GPa]	32(15%)	17	8.9	(6.9)	(5.3)	(4.6)
Lattice parameter, a [Å] (polytype 6H)	3.0815 (0.01%)	3.0874	3.0950	(3.0984)	(3.1021)	(3.1040)
Lattice parameter, c [Å] (polytype 6H)	15.117 (0.02%)	15.144	15.179	(15.194)	(15.210)	(15.218)
Poisson's ratio [ ]	0.16(25%)	0.159	0.157	0.157	0.156	0.156
Shear modulus [GPa]	179(3%)	174	169	167	166	165
Sound velocity, longitudinal [km/s]	11.82(2%)	11.69	11.57	11.52	11.47	11.44
Sound velocity, shear [km/s]	7.52(2%)	7.45	7.38	7.35	7.32	7.31
Specific heat [J kg^{-1} K^{-1}]	715(5%)	1086	1240	1282	1318	1336
Tensile strength [MPa]	250(6%)	250	250	250	250	250
Thermal conductivity [W m^{-1} K^{-1}]	114(8%)	55.1	35.7	31.3	27.8	26.3
Thermal diffusivity [cm^2/s]	0.50(12%)	0.16	0.092	0.079	0.068	0.064
Thermal expansion from 0 °C [10^{-6} K^{-1}]	1.1(10%)	4.4	5.0	5.2	5.4	5.5
Wear coefficient (Log_{10}) [ ] at 0.2 m/s, 5 N	−4.0(5%)	−3.6	−3.6			
Weibull modulus [ ]	11(27%)	11	11	11	11	11

$$\kappa(\mathrm{W\ m^{-1}\ K^{-1}}) = \frac{52\,000\ \mathrm{e}^{-1.24\cdot 10^{-5}T}}{T+437} \pm u_\kappa \quad (14a)$$

$$D(\mathrm{cm^2\ s^{-1}}) = \frac{121\ \mathrm{e}^{-6.98\cdot 10^{-5}T}}{T+219} \pm u_D, \quad (14b)$$

where 0 °C≤T≤2000 °C; u_κ is 12% for T≤400 °C and 8% for T>400 °C; and u_D is 17% for T≤400 °C and 12% for T>400 °C.

4. Conclusion

Validated materials property data are essential to advanced product design techniques. A prerequisite to the validation of property data, however, is the establishment of reproducible data as judged by the consistency of independent measurements. This status has been achieved by advanced ceramics only relatively recently. The present work has provided an assessment of the major physical, mechanical, and thermal properties of sintered α-SiC in which boron and carbon are used as sintering aids to produce a dense ceramic with a grain size of (6±2) μm. Property values, interpolation formulas, and combined standard uncertainties have been determined. The results are summarized in Table 3.

5. References

[1] L. Sheppard, Ceram. Ind. **146**, 34 (1996).
[2] Anonymous, Am. Ceram. Soc. Bull. **75**, 28 (1996).
[3] National Materials Advisory Board, *Enabling Technologies for Unified Life-Cycle Engineering of Structural Components* (National Academy Press, Washington, D. C., 1991), Publication NMAB-455.
[4] J. Rumble, Jr. and J. Carpenter, Jr., Adv. Mater. Proc. **142**, 23 (1992).
[5] Metals and Ceramics Information Center, Engineering Property Data on Selected Ceramics, Vol. 2, *Carbides* (Battelle Columbus Laboratories, 1979), Report Number MCIC-HB-07.
[6] R. S. Storm, W. D. G. Boecker, Ch. H. McMurtry, and M. Srinivasan, *Sintered Alpha Silicon Carbide Ceramics for High Temperature Structural Application:* Status Review and Recent Developments, ASME Paper Number 85-IGT-127 (American Society of Mechanical Engineers, New York, 1985).
[7] M. Srinivasan, ''The Silicon Carbide Family of Structural Ceramics, in Treatise on Materials Science and Technology,'' Vol. 29, *Structural Ceramics*, edited by J. B. Wachtman, Jr. (Academic, San Diego, CA, 1989), pp. 99–159.
[8] T. B. Shaffer, ''Engineering Properties of Carbides,'' in *Engineered Materials Handbook,* Vol. 4, *Ceramics and Glasses,* edited by S. J. Schneider, Jr. (ASM International, Materials Park, OH, 1991), pp. 804–811.
[9] R. G. Munro and S. J. Dapkunas, J. Res. Natl. Inst. Stand. Technol. **98**, 607 (1993).
[10] R. F. Davis, J. E. Lane, C. H. Carter, Jr., J. Bentley, W. H. Wadlin, D. P. Griffis, R. W. Linton, and K. L. More, Scanning Electron. Microsc. **III**, 1161 (1984).
[11] M. Kerr, Ind. Ceram. **9**, 192 (1989).
[12] B. N. Taylor and C. E. Kuyatt, *Guidelines for Evaluating and Expressing the Uncertainty of NIST Measurement Results* (NIST, Washington, D. C., 1993), NIST Tech. Nt. 1297.
[13] Z. Li and R. C. Bradt, J. Am. Ceram. Soc. **69**, 863 (1986).
[14] D. J. Green, J. R. Hellmann, and M. F. Modest, ''Physical Property Measurements of High Temperature Composites,'' in *Projects Within the Center for Advanced Materials, December 1, 1989 to February 28, 1990,* edited by J. R. Hellmann and B. K. Kennedy (Pennsylvania State University Press, 1990), pp. 71–90.
[15] N. L. Hecht, G. A. Graves, D. E. McCullum, A. P. Berens, S. Goodrich, J. D. Wolf, J. R. Hoenigman, P. Yaney, D. Grant, and S. Hilton, *Evaluation of Environmental Effects in Toughened Ceramics for Advanced Heat En-*

gines, Investigation of Selected SiC and Si_3N_4 Ceramics (Oak Ridge National Laboratory, 1990), ORNL/Sub/84-00221/2.
[16] C. H. McMurtry, W. D. G. Boecker, S. G. Seshadri, J. S. Zanghi, and J. E. Garnier, Am. Ceram. Soc. Bull. **66**, 325 (1987).
[17] J. E. Lane, C. H. Carter, Jr., and R. F. Davies, J. Am. Ceram. Soc. **71**, 281 (1988).
[18] R. E. Tressler and K. E. Spear, ''Fundamental Studies of Corrosion of Nonoxide Structural Ceramics,'' in *Projects Within the Center for Advanced Materials*, CAM-8904, GRI-90/0024, edited by J. R. Hellmann and B. K. Kennedy (Pennsylvania State University Press, 1990), pp. 125–143.
[19] N. L. Hecht, S. M. Goodrich, L. Chuck, D. E. McCullum, and V. J. Tennery, Am. Ceram. Soc. Bull. **71**, 653 (1992).
[20] C. A. Tracy and G. D. Quinn, Ceram. Eng. Sci. Proc. **15**, 837 (1994).
[21] E. H. Kraft and G. I. Dooher, ''Mechanical Response of High Performance Silicon Carbide,'' Carborundum Company, Research and Development Division, August 1976.
[22] J. R. Hellmann, D. J. Green, M. F. Modest, P. A. Winand, and K. K. Sikka, ''Physical Property Measurements of High Temperature Composites,'' in *Projects Within the Center for Advanced Materials, 1 June 1990 to 31 August 1990*, edited by J. R. Hellmann and B. K. Kennedy (Pennsylvania State University Press, 1990), pp. 95–114.
[23] P. F. Becher, J. Mater. Sci. **19**, 2805 (1984).
[24] A. Ghosh, M. G. Jenkins, K. W. White, A. S. Kobayashi, and R. C. Bradt, J. Am. Ceram. Soc. **72**, 242 (1989).
[25] F. F. Lange, J. Am. Ceram. Soc. **53**, 290 (1970).
[26] J. L. Smialek and N. S. Jacobson, J. Am. Ceram. Soc. **69**, 741 (1986).
[27] X. Dong, S. Jahanmir, and L. K. Ives, Trib. Inter. **28**, 559 (1995).
[28] G. Orange, H. Tanaka, and G. Fantozzi, Ceram. Interr. **13**, 159 (1987).
[29] Q. Zhang and S. Chou, J. Inorg. Mater. **1**, 251 (1986).
[30] D. E. McCullum, N. L. Hecth, L. Chuck, and S. M. Goodrich, Ceram. Eng. Sci. Proc. **12**, 1886 (1991).
[31] K. D. McHenry and R. E. Tressler, J. Am. Ceram. Soc. **63**, 152 (1980).
[32] M. Srinivasan and S. G. Seshadri, ''Application of Single Edge Notched Beam and Indentation Techniques to Determine Fracture Toughness of Alpha Silicon Carbide,'' in *Fracture Mechanics for Ceramics, Rocks, and Concrete*, ASTM STP 745, edited by S. W. Freiman and E. R. Fuller, Jr. (American Society for Testing and Materials, Philadelphia, 1981), pp. 46–68.
[33] T. E. Easler, R. C. Bradt, and R.E. Tressler, J. Am. Ceram. Soc. **64**, 731 (1981).
[34] K. T. Faber and A. G. Evans, J. Am. Ceram. Soc. **66**, C-94 (1983).
[35] G. Quinn, R. Gettings, and J. Kubler, Ceram. Eng. Sci. Proc. **15**, 846 (1994).
[36] J. C. Conway, Jr., J. J. Mecholsky, Jr., S. M. Wiederhorn, O. M. Jadaan, D. L. Shelleman, and D. C. Cranmer, ''Test Methodology for Tubular Components,'' in *Projects Within the Center for Advanced Materials, 1 September 1989 to 30 November 1989*, edited by J. R. Hellmann and B. K. Kennedy (Pennsylvania State University Press, 1989), pp. 141–160.
[37] S. M. Wiederhorn, D. C. Cranmer, and R. F. Krause, Jr., ''Test Methodology for Tubular Components,'' in *Projects Within the Center for Advanced Materials*, CAM-9002, GRI-90/0205, edited by J. R. Hellmann and S. R. Nestlerode (Pennsylvania State University Press, 1991), pp. 333–360.
[38] R. L. Allor and S. Jahanmir, Am. Ceram. Soc. Bull. **75**, 40 (1996).
[39] E. Rabinowicz, Prod. Eng. **19**, 71 (1958).
[40] S. M. Hsu, D. S. Lim, Y. S. Wang, and R. G. Munro, Lubr. Eng. **47**, 49 (1991).
[41] C. S. Yust and F. J. Carignan, ASLE Trans. **28**, 245 (1984).
[42] M. G. Gee, C. S. Matharu, E. A. Almond, and T. S. Eyre, Wear **138**, 169 (1990).
[43] J. Denape and J. Lamon, J. Mater. Sci. **25**, 3592 (1990).
[44] Engineering Property Data on Selected Ceramics, Vol. 2, *Carbides*, Report Number MCIC-HB-07 (Battelle, Columbus, OH, 1979), p. 5.2.3-2.
[45] R. Morrell, *Handbook of Properties of Technical and Engineering Ceramics*, Part 1: *An Introduction for the Engineer and Designer* (Her Majesty's Stationery Office, London, 1985), p. 75.
[46] Y. Fujisawa, K. Matsusue, and K. Takahara, J. Soc. Mater. Sci. Jpn. **35**, 1112 (1986).
[47] P. T. B. Shaffer, ''Engineering Properties of Carbides,'' in *Engineered Materials Handbook*, Vol. 4, *Ceramics and Glasses*, edited by S. J. Schneider, Jr. (ASM International, Materials Park, OH, 1991), pp. 804–811.
[48] M. E. Schlesinger, ''Melting Points, Crystallographic Transformation, and Thermodynamic Values,'' in *Engineered Materials Handbook*, Vol. 4, *Ceramics and Glasses*, edited by S. J. Schneider, Jr. (ASM International, Materials Park, OH, 1991), pp. 883–891.
[49] C. H. McMurtry, W. D. G. Boecker, S. G. Seshadri, J. S. Zanghi, and J. E. Garnier, Am. Ceram. Soc. Bull. **66**, 325 (1987).
[50] E. H. Kraft and J. A. Coppola, ''Thermo-mechanical Properties of Sintered Alpha Silicon Carbide,'' Carborundum Company, Research and Development Division, March 25 1977.
[51] J. R. Hellmann, D. J. Green, and M. F. Modest, ''Physical Property Measurements of High Temperature Composites,'' in *Projects Within the Center for Advanced Materials, September 1, 1990 to November 30, 1990*, edited by J. R. Hellmann and B. K. Kennedy (Pennsylvania State University Press, 1990), pp. 75–87.